Journal of Microbiological Methods 164 (2019) 105680

Contents lists available at ScienceDirect

Journal of Microbiological Methods

journal homepage: www.elsevier.com/locate/jmicmeth

Fast fluorometric enumeration of *E. coli* using passive chip

Esin Nagihan Kasap[a], Üzeyir Doğan[a], Ferah Çoğun[b], Ender Yıldırım[b], İsmail Hakkı Boyacı[c], Demet Çetin[d], Zekiye Suludere[e], Uğur Tamer[a,*], Nusret Ertaş[a,*]

[a] Gazi University, Faculty of Pharmacy, Department of Analytical Chemistry, 06330, Etiler, Ankara, Turkey
[b] Cankaya University, Department of Mechanical Eng., 06790 Etimesgut, Ankara, Turkey
[c] Hacettepe University, Faculty of Eng., Department of Food Engineering, 06800 Beytepe, Ankara, Turkey
[d] Gazi University, Gazi Faculty of Education, Department of Mathematics and Science Education, 06500 Beşevler, Ankara, Turkey
[e] Gazi University, Faculty of Science, Department of Biology, 06500 Beşevler, Ankara, Turkey

ARTICLE INFO

Keywords:
E. coli
Microfluidic chip
Immunomagnetic separation
Fluorescence
Sandwich immunoassay

ABSTRACT

In this report, a passive microfluidic chip design was developed for fast and sensitive fluorometric determination of *Escherichia coli* (*E. coli*) based on sandwich immunoassay. Initially, magnetic nanoparticles (MNPs) and chitosan modified mercaptopropionic acid capped cadmium telluride (CdTe) quantum dots (QDs) were functionalized with *E.coli* specific antibody to form a sandwich immunoassay with the *E. coli*. The magnetic separation and preconcentration of the *E.coli* from the sample solution was performed in the vial. Conjugation of QDs to the magnetically captured *E. coli* and washing were performed using a passive type of microchip. The microfluidic chip consists of four microchambers connected to each other by microchannels which act as capillary valves. Signal measurement was performed at the last chamber by using a hand-held spectrofluorometer equipped with a fiber optic reflection probe. The selectivity of the method was tested with *Enterobacter aerogenes (E. aerogenes) and Salmonella enteritidis (S. enteritidis),* it was observed that these bacteria have no interference effect on *E.coli* determination. The calibration curve was found to be linear in the range of 10^1–10^5 cfu/mL with a correlation coefficient higher than 0.99. The limit of detection was calculated as 5 cfu/mL. The method was successfully applied to spiked tap and lake water samples. The results suggest that the developed method is applicable for on-site *E. coli* detection and offers several advantages such as large dynamic range, high sensitivity, high selectivity and short analysis time.

1. Introduction

Diseases caused by pathogenic bacteria are significant in that they pose a threat to public health (Morens et al., 2004; Lazcka et al., 2007; Mairhofer et al., 2009). Therefore, rapid detection and identification of bacteria is crucial in order to prevent their quick spreading. Conventional microbial culturing based methods used for bacterial identification are accepted as the standard methods. Although culture testing has long been the discipline's most common method for enumerating bacteria, it has several serious limitations including, inability to detect viable but not culturable bacteria, multi-day incubation periods and the need to verify positive culture results with confirmation testing. Up to now, various techniques such as polymerase chain reaction (PCR) (Suo et al., 2010), quartz crystal microbalance (QCM) (Farka et al., 2015), surface plasmon resonance (SPR) (Torun et al., 2012), electrochemical impedance spectroscopy (EIS) (Li et al., 2015), surface enhanced Raman scattering (SERS) (Zhou et al., 2015; Guven et al., 2011) and fluorescence spectroscopy (Dudak and Boyaci, 2008; Zhu et al., 2011; Dogan et al., 2016) have been reported in the literature for rapid detection of bacteria. Although much progress has been achieved, there is still an urgent need to develop selective, sensitive and rapid methods which is also suitable for on-site detection of bacteria (Law et al., 2015).

In recent years, flow-based biosensor applications have attracted much attention as they reduce laboratory procedures and enable more automated determinations (Phurimsak et al., 2014a). Generally, continuous flow chips are preferred for magnetic particle based assays (Lee et al., 2014; Phurimsak et al., 2014b; Lee et al., 2012). In such chips, working fluids flowing through separate channels merge at a junction where they are mixed with a micro-mixer. However, this procedure may require the use of external tubing, connection ports and pumps to ensure continuous flow of the working fluids. The existence of these peripheral components reduces the reliability of the assay and makes it difficult to operate the chip-based assay. An alternative approach is to utilize pipette operated passive microfluidic chips where working fluids

* Corresponding authors.
E-mail addresses: utamer@gazi.edu.tr (U. Tamer), nertas@gazi.edu.tr (N. Ertaş).

https://doi.org/10.1016/j.mimet.2019.105680
Received 18 March 2019; Received in revised form 31 July 2019; Accepted 1 August 2019
Available online 02 August 2019

are kept stagnant in a series of chambers separated by an immiscible fluid layer (Berry et al., 2012) or by capillary barriers (Phurimsak et al., 2014a; Gliere and Delattre, 2006). Oil is used to separate the chambers of aqueous solutions in a streamline, while the working fluids in neighboring chambers are in direct contact (Phurimsak et al., 2014a). Phaseguides which are shallow ridges acting as capillary barriers patterned on the base of the chip were utilized to obtain the lanes of liquids (Vulto et al., 2011; Yildirim et al., 2014).

Recently, there has been growing interest in quantum dots (QDs) and magnetic nanoparticle (MNP) applications. (Reddy et al., 2006, 2008, 2009; Hassan et al., 2014; Small Methods, 2018; Zhang et al., 2019). Among the other inorganic and carbon based QDs, CdTe QDs have the advantages such as: narrow emission bands, high quantum yield, easy to synthesis and more suitable for the multiplex applications (Petryayeva et al., 2012).

To date, the immunomagnetic separation combined with QD labeled antibodies have been used for bacteria detection. As an example, Su and Li (2004) used CdSe/ZnS QDs and MNP to develop a sandwich type immunoassay method for determination of *E. coli*. In their work, fluorescence signals were measured on a fiber optic fluorescence spectrometer. In another study, streptavidin-coated QDs and MNP were modified with antibody selective to *S. aureus*, and fluorescence measurements were performed using a spectrometer equipped with a fiber optic probe (Hu et al., 2014). The working range and limit of detection of the method was reported as 1×10^3–1×10^6 cfu/mL and 1×10^3 cfu/mL, respectively. The analysis time was approximately three hours. In another work, (Kim et al., 2015) immunomagnetic separation of *Salmonella* on a PDMS microfluidic chip was described. In the first stage, antibody modified MNPs were interacted with the bacteria followed by interaction with CdSe/ZnS QDs in the microfluidic device. Samples were delivered to the system via syringe pump. The fluorescence signals from the complexes were measured using a custom-made fluorometer. The linear range and LOD were determined as 10^3–10^6 cfu/mL and 10^3 cfu/mL, respectively. The proposed method has also been successfully applied in real matrix.

To the best of our knowledge, the combination of magnetic separation and chitosan modified QDs labeling for *E.coli* detection in water samples by using a passive type microfluidic platform has not been reported in the literature previously. Here, we describe a rapid isolation and quantitative analysis method for *E.coli* with QD probe. After immunomagnetic separation of *E.coli*, the homogeneous sandwich structure was formed in passive chip, and fluorescence signals were recorded. The working fluid is transferred into the chip by using a pipette and kept stationary in micro chambers in the chip. The main advantages of the proposed method are: (i) the time necessary for labeling and washing step was decreased, (ii) since the need for an external pump was eliminated, the system is simple and portable and (iii) the consumption of MNP and QD is minimized.

2. Material and methods

2.1. Reagents

All chemicals listed below were of analytical grade and were used as received without any further purification. Cadmium (II) chloride (CdCl2), Trisodium citrate dihydrate ($Na_3C_6H_5O_7{\cdot}2H_2O$), Mercaptopropionic acid (MPA), Hydrogen tellurite (H_2TeO_4). Chitosan, Silver nitrate ($AgNO_3$), iron (II) sulfate heptahydrate ($FeSO_4{\cdot}7H_2O$), sodium hydroxide (NaOH), perchloric acid ($HClO_4$), Sodium borohydride ($NaBH_4$), Iron (III) chloride ($FeCl_3$), Hydrogen tetrachloroaurate ($HAuCl_4$), Hexadecyltrimethylammonium bromide (CTAB), 11-mercaptoundecanoic acid (11-MUA), Ethanolamine, N-(3-dimethylaminopropyl)-N′-ethyl carbodiimide hydrochloride (EDC), Ethylenediaminetetraacetic acid (EDTA), Hydroxylamine hydrochloride, 2-morpholinoethanesulphonic acid monohydrate (MES), Absolute ethanol, NaCl, Na_2HPO4, KH_2PO_4 used as phosphate-buffered saline (PBS) and N-Hydroxysulfosuccinimide sodium salt (NHS). Polyclonal *E. coli* antibody was obtained from Fitzgerald Industries International (Acton, Massachusetts, USA). Immunopure avidin was purchased from Pierce Biotechnology (Rockford, IL). In order to reach the desired concentrations, all solutions were prepared using deionized water (0.06 μS cm^{-1}) obtained from Millipore milli-Q water purification system.

2.2. Chip fabrication

Designed chips were fabricated on polymethyl methacrylate (PMMA) substrates by milling on ProLight WPLM1000 machining center. After the milling process, through holes were drilled using 1 mm milling cutter to open the access holes. In order to seal the channels and the chambers, a blank PMMA sheet was bonded by solvent assisted thermo-compression (Ogilvie et al., 2010). After solvent (chloroform) vapor treatment, PMMA substrates were bonded by applying 270 N/cm^2 pressure for 3 min. at 85 °C. Fig. S1 illustrates the fabrication process.

2.3. Apparatus

Fluorescence measurements were performed using Ocean Optics HR 4000 spectrometer (FL, USA) equipped with a 295 nm LED lamp as an excitation source and a fiber optic reflection probe (Premium-grade reflection probe, Ocean Optics FL, USA). (Fig. S2). The reflection probe has a 6-around-1 fiber bundle design (400 μm core diameter) and a 6-fiber leg is connected to light source, while a single-fiber leg is connected to spectrometer. The spectra were obtained using 750 ms integration time and an average of ten spectra was used to improve signal to noise ratio. A homemade measurement cell containing a room for microchip and a hole for the probe was used to eliminate the background light. Optical absorption spectra were obtained with a Spectronics, Genesis model single beam UV-VIS spectrophotometer. Transmission electron microscopic analyses were performed with JEOL JEM 1400 instrument at 80 kV and 90 kV.

2.4. Microorganism

E. coli (ATCC35218), *S. enteritidis* (ATCC BAA1045) and *E. aerogenes* (ATCC13048) were purchased from Hacettepe University Food Research Center Culture Collection, Ankara, Turkey. The cultures for assay were grown on Tryptic Soy Broth (TSB; Merck, Germany) at 37 °C for 18 h. Cells were then centrifuged at 1377 ($m.s^{-2}$) for 10 min, and supernatant was discarded. Cells were washed three times with sterile PBS (0.67 M at pH 7.4). Turbidity of the cells was adjusted to 0.5 McFarland standard, and bacteria dilutions were prepared making necessary dilutions with sterile PBS.

2.5. Synthesis and surface modification of MPA-CdTe quantum dots with chitosan

An aliquot of 0.100 g of trisodium citrate was dissolved in 25.0 mL, 0.64 mM $CdCl_2$ solution and was transferred to a single neck balloon. Then, 100 μL of 11.5 M mercaptopropionic acid (MPA), 0.010 mmol Te (IV) (pH 8–9) and 50 mg of solid $NaBH_4$ were added sequentially while stirring was maintained. The solution was stirred at 96 °C for 1 h, after which it was cooled to room temperature, and 75 mL of ethanol was added to precipitate the QDs. The supernatant was discarded and the precipitate was washed with 25 mL of ethanol, and the residue was dried at 40 °C. Then, 75 mg of dried precipitate was dissolved in deionized water and diluted to 25.0 mL (3 mg/mL QD). The emission maximum of the QD solution is around 505 nm with relatively low intensity. In order to increase emission intensity and shift the maximum emission wavelength to 550–575 nm, the pH of the final solution was adjusted to 11.4 and heated at 96 °C until the desired emission

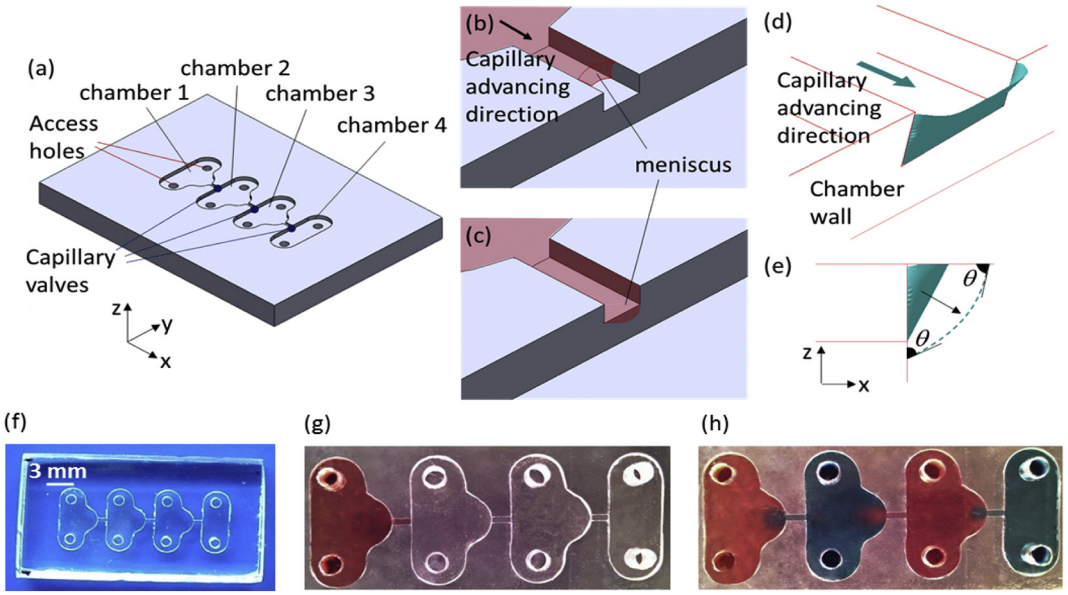

Fig. 1. (a) General view of the microfluidic chip showing the chambers, access holes, and the capillary valves. Chip cover is suppressed for clarity. (b-c) Detailed view of capillary valve. The meniscus advances through the connection channel until it gets pinned at the capillary valve. (d-e) The shape of the pinned meniscus obtained by using Surface Evolver. Breaching of the capillary valve would require a convex interface because of the contact angle between PMMA and aqueous solutions (θ being approximately equal to 70°) as illustrated in (e). (f) Fabricated chip. (g) Liquid gets pinned at the capillary valve between the first and the second chambers as the first chamber is filled. (h) The chip after filling all the chambers. A minor mixing is observed at the capillary valves.

wavelength was reached.

For the 5.0 mL QD solution, 100 µL of 1% (*w/v*) chitosan solution (0.1 g of chitosan was dissolved in 10.0 mL of 1% ((v/v) acetic acid) was added and vortexed for 1 min. The pH of this solution was adjusted to 6 and sonicated for 15 min. Then the solution was centrifuged and the supernatant was discarded, after which it was dispersed in 5 mL MES buffer (pH 6.5). The characterization of the QD and chitosan modified QD was carried out by TEM, X-ray photoelectron spectroscopy, fluorescence and IR spectroscopy in our previous study. (Dogan et al., 2016).

2.6. Preparation of QD-antibody conjugates

In order to activate the amine groups on chitosan-CdTe QDs, 4 mg of EDC and 4 mg of NHS were added to 1.0 mL of the chitosan-modified QD solution and incubated on the orbital shaker for 30 min. The solution was centrifuged for 4 min at 1377 ($m.s^{-2}$), and the supernatant solution was discarded to remove NHS and EDC. This procedure was repeated three times with MES buffer having a pH of 6.5. Then, the precipitate was dispersed in PBS buffer and 100 µL of 1 mg/mL avidin was added. The solution was shaken for 30 min on the orbital shaker to attach avidin to the amine groups. After washing with PBS buffer, the solution was treated with ethanolamine to prevent nonspecific interactions. A 100 µL portion of 0.1 mg/mL biotin-bound rabbit anti-*E.coli* polyclonal antibody solution was added, and the avidin-biotinylated antibody interaction was achieved by shaking it on the orbital shaker for 30 min. The solution was washed three times and then dispersed in 1.0 mL of PBS buffer. The full width at half maxima for the QD-antibody conjugates was around 60–65 nm.

2.7. Preparation of MNP-antibody conjugates

The synthesis and characterization of spherical Fe_3O_4@Au magnetic nanoparticles (9 ± 1 nm) was described previously (Tamer et al., 2013; Dogan et al., 2016). The surface of the magnetic nanoparticles was modified with 11-MUA. To this end, 5 mg MNP was dispersed in 1.0 mL of 20 mM 11-MUA solution prepared in ethanol and stirred overnight. Thus, 11-MUA is covalently bound to the gold surface via thiol groups. The excess of 11-MUA was removed by washing three times with MES buffer. The MNPs were re-dispersed in MES buffer (pH 6.5), 4 mg of EDC and NHS were added to this solution and shaken on an orbital shaker for 30 min to activate the carboxylic acid ends of 11-MUA. Then, the washing procedure was performed at least three times to remove excess EDC and NHS from the solution. After activation of the carboxyl groups, 100 µL of 1.0 mg/mL avidin was added to the 1.0 mL of MNP solution and incubated for 30 min on the orbital shaker. In order to prevent nonspecific interactions 1% (*v/v*) ethanolamine was added to this solution and incubated for 30 min on the orbital shaker. After washing step, MNPs were also re-dispersed in 1.0 mL of PBS buffer (pH 7.4), 100 µL of 0.1 mg/mL biotinylated rabbit anti-*E. coli* antibody solution was added and shaken for 30 min on an orbital shaker. The MNP-antibody conjugates were recovered using a magnet, washed three times with PBS buffer and dispersed in 1.0 mL PBS buffer.

2.8. General procedure of the proposed assay

MNP-antibody conjugate (100 µL) was added to different population density of *E. coli* (500 µL) and incubated for 30 min using an orbital shaker at 100 rpm. This biotinylated antibody recognizes all 'O' and 'K' antigenic serotypes of *E. coli* (https://www.fitzgerald-fii.com/e-coli-antibody-biotin-60-e13b.html (accessed 11 July 2019)). The captured *E. coli* were separated magnetically and washed three times with sterile PBS solution to remove unbound *E. coli* and suspended in 500 µL, 0.1 M PBS. The first chamber of the microchip was filled with 15 µL MNP-*E. coli* conjugate, and the second microchamber was filled with QD-antibody conjugate. The third and the last chamber was filled with washing buffer (phosphate buffered saline, pH 7.4). The MNP-*E. coli* conjugates were transferred to the second microchamber through the microchannel and interacted with the QD-antibody for 1 min by using an external magnet. Then, the MNP-*E. coli*-QD conjugates formed in the second microchamber were transferred to the third microchamber, filled with buffer solution, and circulated for 1 min by moving the magnet in order to eliminate unbound QDs. Finally, the washed sandwich structures were transferred to the last microchamber where the fluorescence spectra were recorded using a hand-held spectrometer. The signal intensity at 550 nm corresponding to maximum emission

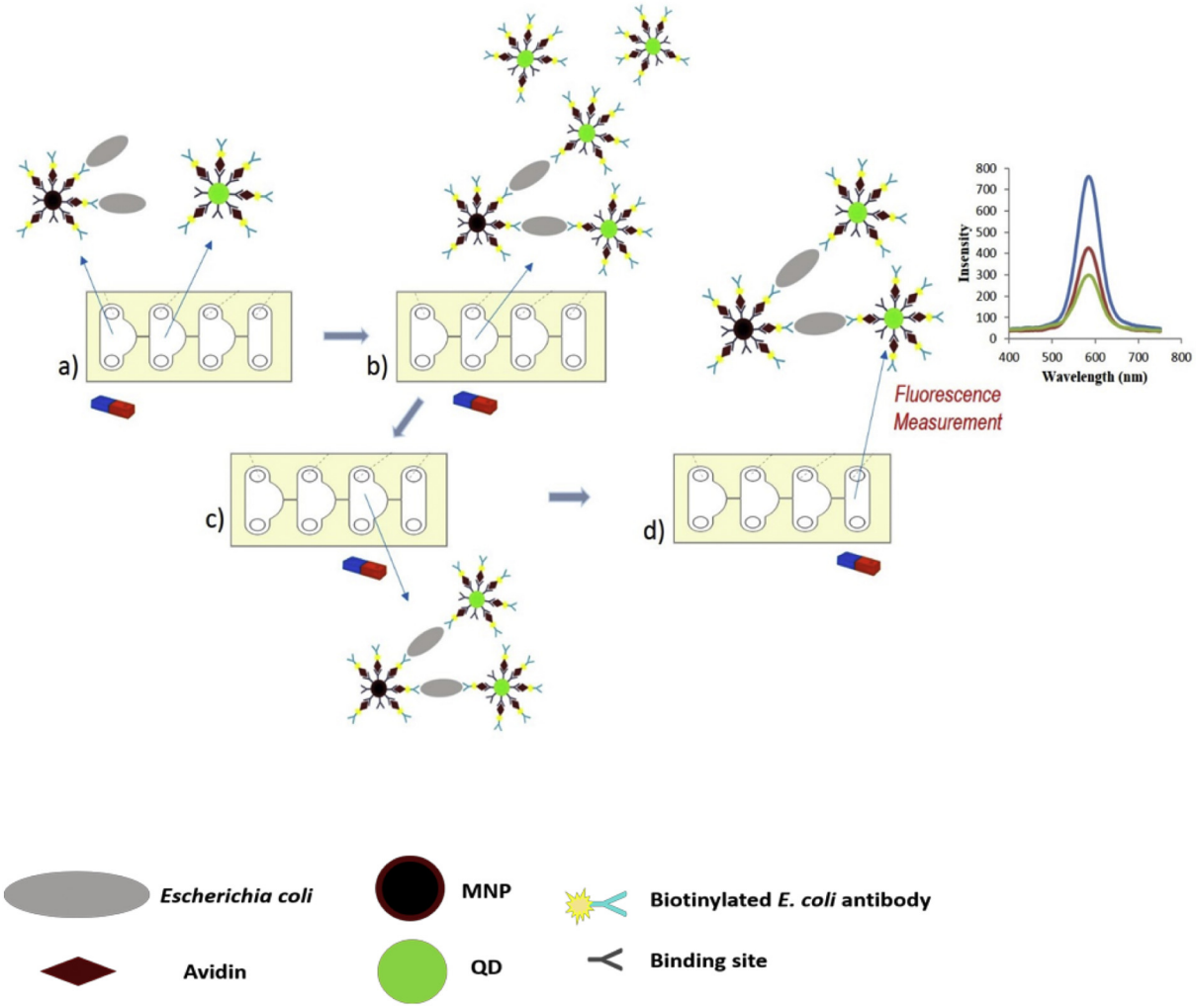

Fig. 2. Schematic illustration of the method a) Manuel injection of MNP-bacteria conjugates and QDs, b) Formation of MNP-bacteria-QD sandwich structure in the second microchamber, c) Washing in the third chamber and d) Fluorescence measurement in the last microchamber, respectively.

wavelength of the QD was followed throughout the study. The schematic representation of the experiment is shown in Fig. 2.

2.9. Sample preparation

As an application, tap water and lake water were analyzed for *E.coli* by using plate counting method and proposed method. Tap water samples (100 mL, $n = 3$) were spiked with 500 µL population densities of 1.2×10^2 cfu/mL and 1.2×10^4 cfu/mL of *E.coli*. 100 µL volume of MNP-antibody conjugate was added and incubated in orbital shaker for 30 min. MNP-*E. coli* conjugates were collected using a magnet, dispersed in 1.0 mL PBS buffer and washed three times. After washing, the MNP-*E. coli* conjugate was dispersed in 500 µL PBS buffer and subjected to the general procedure.

Lake water sample was filtered through 0.45 µm pore size filters and three parallel samples of filtered lake water (10 mL) were spiked with 500 µL of *E. coli* at population densities of 1.2×10^2 and 1.2×10^4 cfu/mL, and the same procedure was applied.

3. Results and discussion

Rapid analysis and identification of bacteria have recently been considered as an important research topic. Conventional methods require copious amounts of solvent and are time-consuming. Furthermore, they require complicated sample preparation steps and expensive reagents (Tokeshi et al., 2003). The use of magnetic nanoparticles to separate the bacteria from their matrix was found to be more effective due to the high surface/volume ratio (Tamer et al., 2011). This approach has provided a higher contact surface area resulting in higher capture efficiency. Our previous work also showed that the magnetic nanoparticle based immunoassay system showed capture efficiency similar to the conventional Dynabeads based immunomagnetic separation (Tamer et al., 2010).

In a recent study, the performance of passive chip was evaluated for quantitative analysis of luteinizing hormone (LH) by using labeled surface enhanced Raman scattering (SERS) probe (Gjergjizi et al., 2018) and C-reactive protein immunoassay fluorescently labeled secondary antibody (Phurimsak et al., 2014b). The present work investigated the fluorescence measurements of QD probe for detection of *E. coli* in a passive microchip, and all the other interactions with modified nanoparticles were performed in a passive microchip. Here, a magnetic particle-based assay platform was used in which *E.coli* bound magnetic particles were transferred sequentially through chambers for labeling and washing. The fluorescence signal from the MNP-*E.coli*-QD conjugates was measured using a hand-held fluorescence spectrometer equipped with a fiber optic reflection probe. The proposed assay consists of three major steps; which are (i) the immobilization of antibodies on Fe_3O_4@Au and QDs NPs; (ii) isolation of *E.coli* from water samples by using Fe_3O_4@Au-antibody, and (iii) labeling the isolated *E.coli* with QD-antibody, washing it with buffer and performing the fluorescence

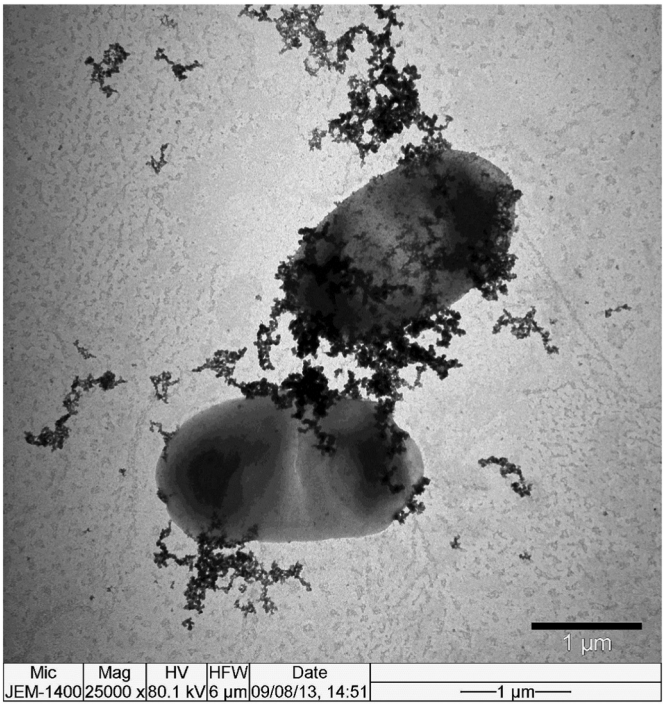

Fig. 3. TEM image of the bacteria removed from the measurement microchamber.

measurement in a passive chip.

3.1. Characteristics of the microfluidic chip

The chip (Fig. 1a) consists of four 3 mm × 6 mm chambers connected by 400 µm wide channels. The depth of the channels (200 µm) was designed to be less than the depth of the chambers (500 µm) so that the exit of a channel to a neighboring chamber could act as a capillary barrier. Each chamber has two access holes. Working liquids were pipetted to the chambers in sequence through one of these access holes. After transferring the liquid to the first chamber, it flows through the connection channel by capillary action (Fig. 1b–c). When the capillary interface reaches to the exit of the channel, the liquid cannot flow any further due to meniscus pinning (Gjergjizi et al., 2018; Cho et al., 2007; Atencia and Beebe, 2005; Chen et al., 2011). Beyond this point, due to negative concavity of the capillary interface (Fig. 1d–e), advancing of the flow can only be possible by pressurizing the chamber. Fig. 1d illustrates the shape of the meniscus pinned at the capillary valve obtained through Surface Evolver software (Brakke, 2013; Zhao et al., 2001). After filling the first chamber, the rest of the chambers could be filled similarly in sequence.

The fabricated chips (Fig. 1f) were initially tested to verify the operation of the capillary valves. For this purpose, dyed water was sequentially pipetted into the chambers. Initial flow test results are shown in Fig. 1g and h. During the tests, it was observed that while filling the next chamber, a minor back flow occurred in the previous channel, which caused a local mixing of the working liquids. However, this minor mixing problem did not affect the test results. The chips were also tested with magnetic particles. During the magnetic particle tests, it was observed that the traces of magnetic particles stuck on the channel and chamber surfaces. In order to solve this problem, hydrophilicity of the chips was improved by exposing them to air plasma for 1 min after the bonding process. After each use, the microchips were cleaned in water by sonication for 10 min. Then, ethanol was passed through the microchambers with a pipette and dried at 40 °C for 12 h. A microchip could be used more than ten times.

3.2. Optimization of experimental parameters

The experimental parameters such as the amount of MNP-antibody to be used for capturing *E. coli*, the final population densities of the magnetically enriched MNP-antibody-*E. coli* and QD-antibody conjugates to be loaded into the microchip were optimized to obtain the highest fluorescence signal.

The amount of MNP-antibody conjugate should be at a concentration that is high enough to capture all the *E. coli* but does not cause any aggregation. Since avidin: MNP ratio is 10:1 and the size of the avidin is about 7 nm, we estimated maximum four biotinylated antibody per particle. In order to optimize the amount of MNP, 50, 75 and 100 µL volume of MNP-antibody complex was added to 500 µL of 1×10^3 cfu/mL *E. coli* solution and incubated as described previously. The highest fluorescence intensity was obtained with 100 µL volumes of MNP-antibody conjugate, which was selected and used throughout the study (Supplementary data, Fig. S3). Similarly, after the *E. coli* capturing and washing steps, the concentration of MNP-antibody-*E. coli* conjugates loaded into the microchip was studied using different dilution volumes of 500, 750 and 1000 µL with PBS. As expected, the minimum dilution volume gave the highest fluorescence intensity; therefore, 500 µL, dilution volume was selected (Fig. S4). The concentration of QD-antibody

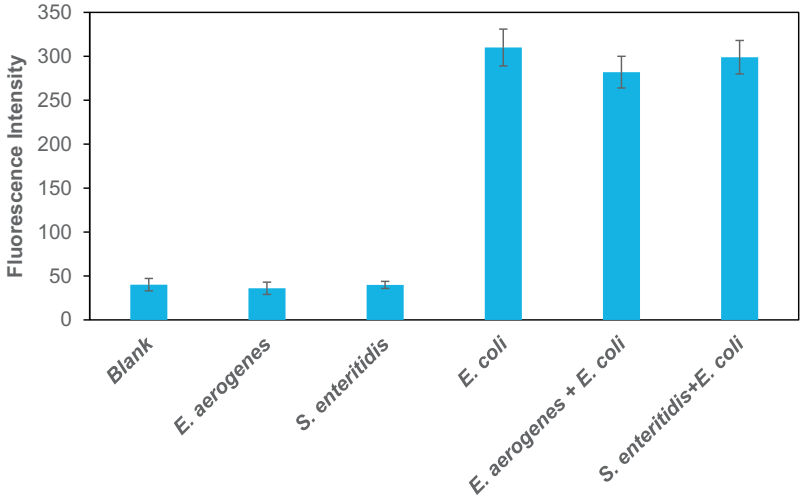

Fig. 4. The fluorescence emission intensities measured for Blank, *E. aerogenes, S. enteritidis* (6×10^6 cfu/mL), *E. coli* (1×10^4 cfu/mL), *E. aerogenes* and *E. coli, S. enteritidis* spiked with 1×10^4 cfu/mL *E. coli*; respectively.

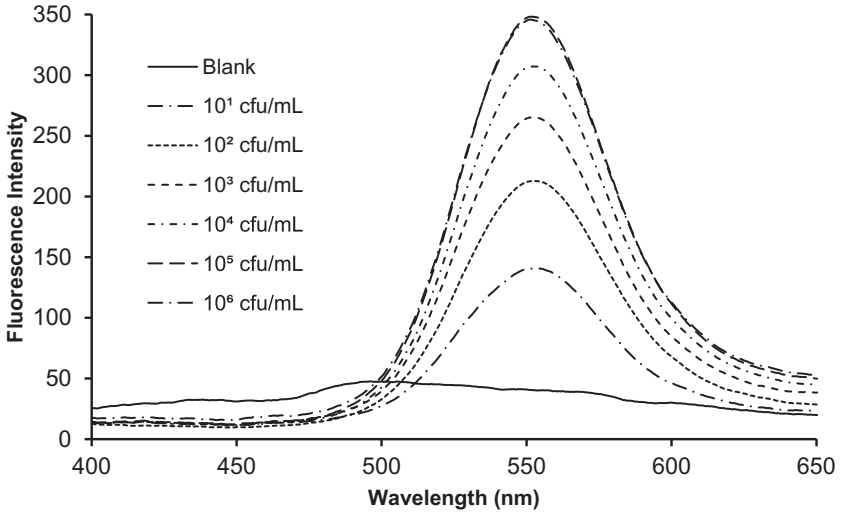

Fig. 5. Fluorescence emission spectra obtained from the microchip for calibration; integration time 750 ms, the signals are the average of the three parallel microchip.

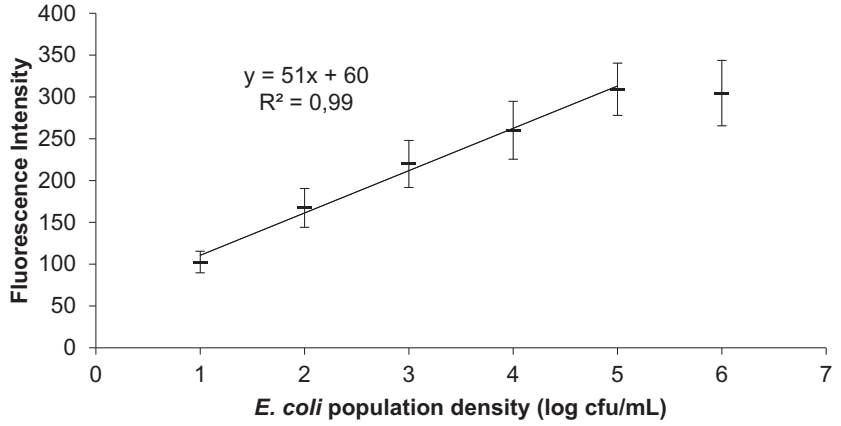

Fig. 6. Fluorescence intensity as a function of *E. coli* population density. Each point is the average of the three parallel microchips.

Table 1
Determination of *E.coli* in water samples.

	E. coli (cfu/mL)			
	Added	Found	Added	Found
Tap water	120	100 ± 17	$1{,}2 \times 10^4$	1,2 ± 0,1 ($\times 10^4$)
Lake water	120	80 ± 30	$1{,}2 \times 10^4$	1,1 ± 0,4 ($\times 10^4$)

conjugate loaded to the second microchamber was also optimized since the fluorescence intensity is directly proportional to QD concentration. An aliquot of 15 µL of the QD-antibody conjugate dispersed in 300, 500 and 750 µL PBS were loaded to the second microchamber, and the general procedure was applied. The highest fluorescence signal was observed using QD-antibody conjugate dispersed in 300 µL and used throughout the study (Fig. S5). Each data are the mean values of the fluorescence intensity obtained with three parallel microchips.

3.3. Characterization of the proposed method for E.coli detection

The number of scans and integration time were set to 10 and 750 ms, respectively. These settings were used throughout the study since higher scan number and integration times caused increase in background signal.

The measurements with blank and standards confirm that the QD fluorescence signal at 550 nm was observed only in the presence of *E. coli*. In order to prove that the signal stemmed from the MNP-*E. coli*-QD conjugates, 1.0×10^3 cfu/mL *E.coli* was incubated with 100 µL MNP-antibody for 30 min, washed and diluted to 500 µL with PBS. After the general procedure and fluorescence measurement from the microchip, the sample solution collected from the measurement microchamber was analyzed using TEM. The TEM image (Fig. 3) clearly indicated the presence of *E. coli* surrounded by MNP and QD in the measurement microchamber.

3.4. Selectivity test and sample analysis

In order to test the nonspecific interactions between bare MNP and QDs, the general procedure was repeated without antibody modification of MNP and QD, in the presence of 1.0×10^3 cfu/mL of *E. coli.* As shown in Fig. S5, the signal was the same as the blank signal. This indicates that there are no non-specific interactions between bare MNP and QD in the solution.

The selectivity of the method for *E. coli* was evaluated with 6×10^6 cfu/mL of *E. aerogenes* and *S. enteritidis*. Firstly, *E. coli* selective antibody modified MNP was interacted with those bacteria in separate vial. Secondly, same experiment was repeated in the presence of 1×10^4 cfu/mL *E. coli.* Fluorescence signals obtained from 6×10^6 cfu/mL of *E. aerogenes* and *S. enteritidis* were compared with blank signal and spiked samples were compared with 1×10^4 cfu/mL *E.coli* standard

Table 2
Comparison of the developed method with other reported methods for *E.coli* detection.

Technique	Sample	Analysis time (min)	Linear Range (cfu/mL)	LOD (cfu/mL)	Reference
Real-time PCR	Culture	320	5–5×10^4	5 cells	(Fu et al., 2005)
SPR biosensor	Culture	Not available	10^2–10^9	10^2	(Oh et al., 2005)
UV-VIS Microfluidic	Water	Not available	10^1–10^5	10^1	(Lee et al., 2015)
	Milk		10^2–10^5	10^2	
Fluorescence	Water	< 120	8.9×10^1–1.9×10^6	8.9×10^1	(Dudak and Boyaci, 2008)
Fluorescence	Water	< 200	8×10^4–1.6×10^7	Not available	(Dudak et al., 2009)
Fluorescence	Standards	< 120	10^2–10^7	10^2	(Xue et al., 2009)
Fluorescence	Standards	< 15	1.3×10^2–1.3×10^3	28	(Carrillo-Carrion et al., 2011)
Fluorescence	Standards	< 30	2.5×10^3–1.95×10^8	5×10^2	(Chen et al., 2011)
Fluorescence	Standards	< 120	10^3–10^7	10^3	(Su and Li, 2004)
Fluorescence	Water	< 120	10^2–10^8	30	(Dogan et al., 2016)
	Urine				
Fluorescence Microfluidic	Chicken extract	70	10^3–10^6	10^3	(Kim et al., 2015)
Fluorescence Microfluidic	Standards	Not available	10^3–10^7	10^3	(Agrawal et al., 2012)
Fluorescence Microfluidic	Standards	120	10^4–10^7	10^4	(Yang and Li, 2006)
Fluorescence Microfluidic	Tap water, Lake water	50	10^1–10^5	5	This work

signal. Three parallel microchip was used for each experiment. As shown in Fig. 4, the fluorescence signal remained unchanged, same as blank signal, for *E. aerogenes* and *S. enteritidis* and the fluorescence signal intensities of *E. aerogenes* and *S. enteritidis* solutions (1×10^6 cfu/mL) both fortified with 1×10^4 cfu/mL *E. coli* were the same with the standard containing only 1×10^4 cfu/mL *E. coli* (Fig. 4). In addition, TEM images were taken after the *E. aerogenes* and *S. enteritidis* were interacted with the biotinylated *E. coli* -specific antibody. As shown in Fig. S7, there was no MNP on *E. aerogenes* and *S. enteritidis* while the *E. coli* was surrounded with MNP. These results suggest the high selectivity of the proposed method for *E. coli* assay.

In order to evaluate the applicability, recovery and possible matrix effect, real samples obtained from lake and tap water were analyzed for *E. coli* by using the developed immunoassay method, and the results were compared with plate counting methods. *E. coli* could not be detected in the samples in both methods. Known population densities of *E. coli* at 1.2×10^2 and 1.2×10^4 cfu/mL were added to water samples and analyzed for *E. coli*. Each sample was studied using three parallel microchips. As shown in Table 1, the recovery for the microchip immunoassay was in the range of 67–98% for the lake and tap water. The results demonstrated that the developed immunoassay could be used for accurate detection of *E. coli* in both water samples.

3.5. Analytical performance of the method

Under the optimized conditions, fluorescence intensity increases with *E.coli* population density. In order to determine the linear range, the modified MNPs were incubated with *E. coli* standard solutions with population densities ranging from 1.0×10^1 to 1.0×10^8 cfu/mL for 30 min, and the general procedure was applied. Three parallel microchips for each population densities were prepared. Fig. 5 shows the mean fluorescence spectra of standard *E. coli* solutions between 1.0×10^1–1.0×10^6 cfu/mL measured from the microchip by using the fiber optic reflection probe. Fig. 6 shows the calibration curve constructed by using the fluorescence intensity at 550 nm. A linear relationship between *E. coli* population density and fluorescence intensity was observed in the range of 1×10^1 to 1×10^5 cfu/mL with a determination coefficient of (R^2) 0.99. The correlation equation was $y = 51\times + 60$, where Y is the fluorescence intensity and X is the population density of *E. coli*. As shown in Fig. 5 and Fig. 6, population densities of 1.0×10^5 and 1.0×10^6 cfu/mL gave the same signal intensity. Experimentally, it was observed that QD was insufficient for *E. coli* population densities of 1.0×10^6 cfu/mL and higher. We have not attempted to increase the QD concentration as the linear range is wide enough for quantitative analysis and the aggregation of MNP-*E. coli*-QD conjugate at higher QD concentrations may clog capillary valves.

The limit of detection was calculated as 5 cfu/mL, using the equation $S_{LOD} = S_{bl} + 3 \times s_{bl}$, where S_{bl} is the mean of blank measurements ($n = 11$), s_{bl} is the standard deviation of blank measurements. The minimum detectable signal (S_{LOD}), calculated from the equation, was converted to population density by using a calibration curve constructed with a series of standards (0, 3, 5, 7 and 10 cfu/mL *E. coli*). Since, this part of the calibration curve was not linear, a polynomial fitting was used for the estimation of LOD. Notably, the sensitivity of the proposed method is significantly lower than that of fluorescent sensors based on quantum dots (Dogan et al., 2016; Su and Li, 2004; Kim et al., 2015; Trietsch et al., 2011; Carrillo-Carrion et al., 2011; Kuang et al., 2013). This high sensitivity might be attributed to the use of a passive microfluidic chip where working fluids are kept stagnant and which allows the use of high scan number with longer integration time. In flow based immunomagnetic assays, loss of analyte in washing and labeling steps is more likely. The precision of the method expressed as relative standard deviation (RSD) was determined ($n = 5$) of 1×10^1 cfu/mL. The percent RSD of the sequential measurements from the same microchip was < 3%, while the % RSD among the parallel microchips was generally < 20%.

The total analysis time, including the capturing of *E. coli* with MNP-antibody, washing steps (approximately 40 min), formation of sandwich structure in the microchip and measurement (approximately 10 min), was < 50 min. As can be seen in Table 2, the analysis time of the developed method is shorter than the other microfluidic fluorosensors previously reported for detection of bacteria. Only one of these studies, in which immunomagnetic separation was not used, reported a shorter analysis time (Trietsch et al., 2011).

4. Conclusion

A passive microfluidic system for fast and sensitive fluorometric determination of *E. coli* based on sandwich immunoassay was demonstrated in the present study. The main advantage of the developed method is its simplicity. The use of passive microfluidic chip design allows labeling with QD and subsequent washing steps to be done quickly and easily. The chemicals and sample volumes used during experiment was minimized by using passive microfluidic chip. This is particularly important because it reduces the consumption of MNP and QD, which take time to synthesize and modify. The selectivity of the method was tested using different bacteria such as *E. aerogenes, S. enteritidis* and their signal intensities were found to be the same as blank signal. The developed assay can be applied for determination of *E. coli* in water samples with good recovery values. In addition to the high sensitivity and selectivity of the method, the instrumentation is simple and portable, which makes the proposed method suitable for remote analysis.

Declaration of Competing Interest

There are no conflicts of interest to declare.

Acknowledgment

This work was supported by the Scientific and Technological Research Council of Turkey (TUBITAK) with grant number 114Z408.

Appendix A. Supplementary data

Supplementary data to this article can be found online at https://doi.org/10.1016/j.mimet.2019.105680.

References

Agrawal, S., Morarka, A., Bodas, D., Paknikar, K.M., 2012. Multiplexed detection of waterborne pathogens in circular microfluidics. Appl. Biochem. Biotechnol. 167 (6), 1668–1677.
Atencia, J., Beebe, D.J., 2005. Controlled microfluidic interfaces. Nature. 437 (7059), 648–655.
Berry, S.M., Maccoux, L.J., Beebe, D.J., 2012. Streamlining immunoassays with immiscible filtrations assisted by surface tension. Anal. Chem. 84 (13), 5518–5523.
Brakke, K.A., 2013. Surface Evolver Manual.
Carrillo-Carrion, C., Simonet, B.M., Valcarcel, M., 2011. Colistin-functionalised CdSe/ZnS quantum dots as fluorescent probe for the rapid detection of Escherichia coli. Biosens. Bioelectron. 26 (11), 4368–4374.
Chen, H., Abolmatty, A., Faghri, M., 2011. Microfluidic inverse phase ELISA via manipulation of magnetic beads. Microfluid. Nanofluid. 10 (3), 593–605.
Cho, H., Kim, H.Y., Kang, J.Y., Kim, T.S., 2007. How the capillary burst microvalve works. J. Colloid Interface Sci. 306 (2), 379–385.
Dogan, U., Kasap, E., Cetin, D., Suludere, Z., Boyaci, I.H., Turkyilmaz, C., Ertas, N., Tamer, U., 2016. Rapid detection of bacteria based on homogenous immunoassay using chitosan modified quantum dots. Sensor Actuat B-Chem. 233, 369–378.
Dudak, F.C., Boyaci, I.H., 2008. Enumeration of immunomagnetically captured Escherichia coli in water samples using quantum dot-labeled antibodies. J. Rapid. Meth. Aut. Mic. 16 (2), 122–131.
Dudak, F.C., Boyaci, I.H., Jurkevica, A., Hossain, M., Aquilar, Z., Halsall, H.B., Seliskar, C.J., Heineman, W.R., 2009. Determination of viable Escherichia coli using antibody-coated paramagnetic beads with fluorescence detection. Anal. Bioanal. Chem. 393 (3), 949–956.
Farka, Z., Kovar, D., Skladal, P., 2015. Rapid detection of microorganisms based on active and passive modes of QCM. Sensors-Basel. 15 (1), 79–92.
Fitzgerald Industries International, USA https://www.fitzgerald-fii.com/e-coli-antibody-biotin-60-e13b.html.
Fu, Z., Rogelj, S., Kieft, T.L., 2005. Rapid detection of Escherichia coli O157:H7 by immunomagnetic separation and real-time PCR. Int. J. Food Microbiol. 99 (1), 47–57.
Gjergjizi, B., Cogun, F., Yildirim, E., Eryilmaz, M., Selbes, Y., Saglam, N., Tamer, U., 2018. SERS-based ultrafast and sensitive detection of luteinizing hormone in human serum using a passive microchip. Sensor Actuat B-Chem. 269, 314–321.
Gliere, A., Delattre, C., 2006. Modeling and fabrication of capillary stop valves for planar microfluidic systems. Sensor Actuat a-Phys. 130, 601–608.
Guven, B., Basaran-Akgul, N., Temur, E., Tamer, U., Boyaci, I.H., 2011. SERS-based sandwich immunoassay using antibody coated magnetic nanoparticles for Escherichia coli enumeration. Analyst. 136 (4), 740–748.
Hassan, M., Haque, E., Reddy, K.R., Minett, A.I., Chen, J., Gomes, V.G., 2014. Edge-enriched graphene quantum dots for enhanced photo-luminescence and super-capacitance. Nanoscale. 6, 11988–11994.
Hu, Y.H., Wang, C.C., Bing, B., Li, M.T., Wang, R.H., Li, Y.B., 2014. Detection of staphylococcus aureus using quantum clots as fluorescence labels. Int J Agr Biol Eng. 7 (1), 77–83.
Kim, G., Moon, J.H., Moh, C.Y., Lim, J.G., 2015. A microfluidic nano-biosensor for the detection of pathogenic Salmonella. Biosens. Bioelectron. 67, 243–247.
Kuang, H., Cui, G., Chen, X.J., Yin, H.H., Yong, Q.Q., Xu, L.G., Peng, C., Wang, L., Xu, C., 2013. A one-step homogeneous sandwich immunosensor for Salmonella detection based on magnetic nanoparticles (MNPs) and quantum dots (QDs). Int. J. Mol. Sci. 14 (4), 8603–8610.
Lazcka, O., Del Campo, F.J., Munoz, F.X., 2007. Pathogen detection: a perspective of traditional methods and biosensors. Biosens. Bioelectron. 22 (7), 1205–1217.
Lee, H., Xu, L.F., Ahn, B., Lee, K.S., Oh, K.W., 2012. Continuous-flow in-droplet magnetic particle separation in a droplet-based microfluidic platform. Microfluid. Nanofluid. 13 (4), 613–623.
Lee, H., Xu, L.F., Oh, K.W., 2014. Droplet-based microfluidic washing module for magnetic particle-based assays. Biomicrofluidics. 8 (4).
Lee, W., Kwon, D., Choi, W., Jung, G.Y., Au, A.K., Folch, A., Jeon, S., 2015. 3D-printed microfluidic device for the detection of pathogenic Bacteria using size-based separation in Helical Channel with trapezoid cross-section. Sci Rep-Uk. 5, 7717.
Li, Z.M., Fu, Y.C., Fang, W.H., Li, Y.B., 2015. Electrochemical impedance immunosensor based on self-assembled monolayers for rapid detection of *Escherichia coli* O157:H7 with signal amplification using lectin. Sensors-Basel. 15 (8), 19212–19224.
Mairhofer, J., Roppert, K., Ertl, P., 2009. Microfluidic Systems for Pathogen Sensing: a review. Sensors-Basel. 9 (6), 4804–4823.
Morens, D.M., Folkers, G.K., Fauci, A.S., 2004. The challenge of emerging and re-emerging infectious diseases. Nature. 430 (6996), 242–249.
Ogilvie, I.R.G., Sieben, V.J., Floquet, C.F.A., Zmijan, R., Mowlem, M.C., Morgan, H., 2010. Reduction of surface roughness for optical quality microfluidic devices in PMMA and COC. J. Micromech. Microeng. 20 (6).
Oh, B.K., Lee, W., Chun, B.S., Bae, Y.M., Lee, W.H., Choi, J.W., 2005. The fabrication of protein chip based on surface plasmon resonance for detection of pathogens. Biosens. Bioelectron. 20 (9), 1847–1850.
Petryayeva, E., Algar, W.R., Medintz, I.M., 2012. Quantum dots in bioanalysis: a review of applications across various platforms for fluorescence spectroscopy and imaging. Appl. Spectrosc. 67 (3), 215–253.
Phurimsak, C., Tarn, M.D., Peyman, S.A., Greenman, J., Pamme, N., 2014a. B'. On-Chip determination of C-reactive protein using magnetic particles in continuous flow. Anal. Chem. 86 (21), 10552–10559.
Phurimsak, C., Yildirim, E., Tarn, M.D., Trietsch, S.J., Hankemeier, T., Pamme, N., Vulto, P., 2014b. A'. Phaseguide assisted liquid lamination for magnetic particle-based assays. Lab Chip 14 (13), 2334–2343.
Reddy, K.R., Lee, K.-P., Gopalan, A.I., Kim, M.S., Showkat, A.M., Nho, Y.C., 2006. Synthesis of metal (Fe or Pd)/alloy (Fe–Pd)-nanoparticles-embedded multiwall carbon nanotube/sulfonated polyaniline composites by γ irradiation. J. Polym. Sci. Part A: Polym. Chem. 44, 3355–3364.
Reddy, K.R., Lee, K.-P., Kim, J.Y., Lee, Y., 2008. Self-assembly and graft polymerization route to monodispersed Fe3O4@SiO2—polyaniline Core–Shell composite nanoparticles: physical properties. J. Nanosci. Nanotechnol. 8, 5632–5639.
Reddy, K.R., Park, W., Sin, B.C., Noh, J., Lee, Y., 2009. Synthesis of electrically conductive and superparamagnetic monodispersed ironoxide-conjugated polymer composite nanoparticles byin situchemicaloxidative polymerization. J. Colloid Interface Sci. 335, 34–39.
Small Methods. 2018. 2 (11), 1800050.
Su, X.L., Li, Y.B., 2004. Quantum dot biolabeling coupled with immunomagnetic separation for detection of Escherichia coli O157 : H7. Anal. Chem. 76 (16), 4806–4810.
Suo, B., He, Y.P., Tu, S.I., Shi, X.M., 2010. A multiplex real-time polymerase chain reaction for simultaneous detection of Salmonella spp., Escherichia coli O157, and listeria monocytogenes in meat products. Foodborne Pathog. Dis. 7 (6), 619–628.
Tamer, U., Gündoğdu, Y., Boyacı, I.H., Pekmez, K., 2010. Synthesis of magnetic core-shell Fe3O4-Au, nanoparticles for biomolecule immobilization and detection. J. Nanopart. Res. 12 (4), 1187–1196.
Tamer, U., Boyaci, I.H., Temur, E., Zengin, A., Dincer, I., Elerman, Y., 2011. Fabrication of magnetic gold nanorod particles for immunomagnetic separation and sers application. J. Nanopart. Res. 13 (8), 167–176.
Tamer, U., Cetin, D., Suludere, Z., Boyaci, I.H., Temiz, H.T., Yegenoglu, H., Daniel, P., Dinçer, İ., Elerman, Y., 2013. Gold-coated iron composite nanospheres targeted the detection of *Escherichia coli*. Int. J. Mol. Sci. 14 (3), 6223–6240.
Tokeshi, M., Kikutani, Y., Hibara, A., Sato, K., Hisamoto, H., Kitamori, T., 2003. Chemical processing on microchips for analysis, synthesis, and bioassay. Electrophoresis 24 (21), 3583–3594.
Torun, O., Boyaci, I.H., Temur, E., Tamer, U., 2012. Comparison of sensing strategies in SPR biosensor for rapid and sensitive enumeration of bacteria. Biosens. Bioelectron. 37 (1), 53–60.
Trietsch, S.J., Rauwé, W., Urban, G.A., Manz, A., Hankemeier, T., Linden, H., Vulto, P., 2011. The phaseguide paradigm: priming and emptying of monolithic polymer chips. Micro Total Analysis Syst. 942–944.
Vulto, P., Podszun, S., Meyer, P., Hermann, C., Manz, A., Urban, G.A., 2011. Phaseguides: a paradigm shift in microfluidic priming and emptying. Lab Chip 11 (9), 1596–1602.
Xue, X.H., Pan, J., Xie, H.M., Wang, J.H., Zhang, S., 2009. Fluorescence detection of total count of Escherichia coli and Staphylococcus aureus on water-soluble CdSe quantum dots coupled with bacteria. Talanta. 77 (5), 1808–1813.
Yang, L.J., Li, Y.B., 2006. Simultaneous detection of Escherichia coli O157 : H7 and Salmonella typhimurium using quantum dots as fluorescence labels. Analyst. 131 (3), 394–401.
Yildirim, E., Trietsch, S.J., Joore, J., Van den Berg, A., Hankemeier, T., Vulto, P., 2014. Phaseguides as tunable passive microvalves for liquid routing in complex microfluidic networks. Lab Chip 14 (17), 3334–3340.
Zhang, F., Liu, Y., Ma, P., Tao, S., Sun, Y., Wang, X., Song, D., 2019. A Mn-doped ZnS quantum dots-based ratiometric fluorescence probe forlead ion detection and "off-on" strategy for methyl parathion detection. Talanta. 204, 13–19.
Zhao, B., Moore, J.S., Beebe, D.J., 2001. Surface-directed liquid flow inside microchannels. Science. 291 (5506), 1023–1026.
Zhou, H.B., Yang, D.T., Ivleva, N.P., Mircescu, N.E., Schubert, S., Niessner, R., Wieser, A., Haisch, C., 2015. Label-free in situ discrimination of live and dead bacteria by surface-enhanced Raman scattering. Anal. Chem. 87 (13), 6553–6561.
Zhu, P.X., Shelton, D.R., Li, S.H., Adams, D.L., Karns, J.S., Amstutz, P., Tang, C.M., 2011. Detection of *E. coli* O157:H7 by immunomagnetic separation coupled with fluorescence immunoassay. Biosens. Bioelectron. 30 (1), 337–341.